

## SUMMARY

The goal of this work is to robustly simulate polar ozone ( $O_3$ ) variability during recent years by optimizing a version of the passive ozone subtraction technique. The eventual goal is to predict future polar  $O_3$  loss in a changed climate, and to explore how the atmosphere responds to polar ozone recovery. The passive  $O_3$  subtraction technique subtracts simulated, inert (or partially inert)  $O_3$  from observed or predicted ozone. The work here uses the Specified Dynamics Whole Atmosphere Community Climate Model (SD-WACCM) to simulate a “pseudo”-passive  $O_3$  tracer which only non-halogen chemistry is allowed to perturb. Observations are from the Aura Microwave Limb Sounder (MLS).  $O_3$  loss calculations during Arctic winter 2004/05 are in good agreement with previous work, providing an initial verification that SD-WACCM is appropriate for these types of studies. Diagnostic comparisons to observations of ozone-related species point to minor deficiencies in SD-WACCM simulations of descent and/or mixing, as well as halogen-induced  $O_3$  depletion.

## METHOD

- Three model simulations:
  - full-ozone chemistry
  - gas-phase-ozone chemistry only (pseudo-passive tracer)
  - no ozone chemistry (passive tracer, for reference)
- Inferred  $O_3$  loss:**  $O_3$  loss quantified by model & measurement  
IL = (EOS MLS  $O_3$ ) – (SD-WACCM pseudo-passive  $O_3$ )
- Modeled  $O_3$  loss:**  $O_3$  loss quantified by model only  
ML = (SD-WACCM  $O_3$ ) - (SD-WACCM pseudo-passive  $O_3$ )

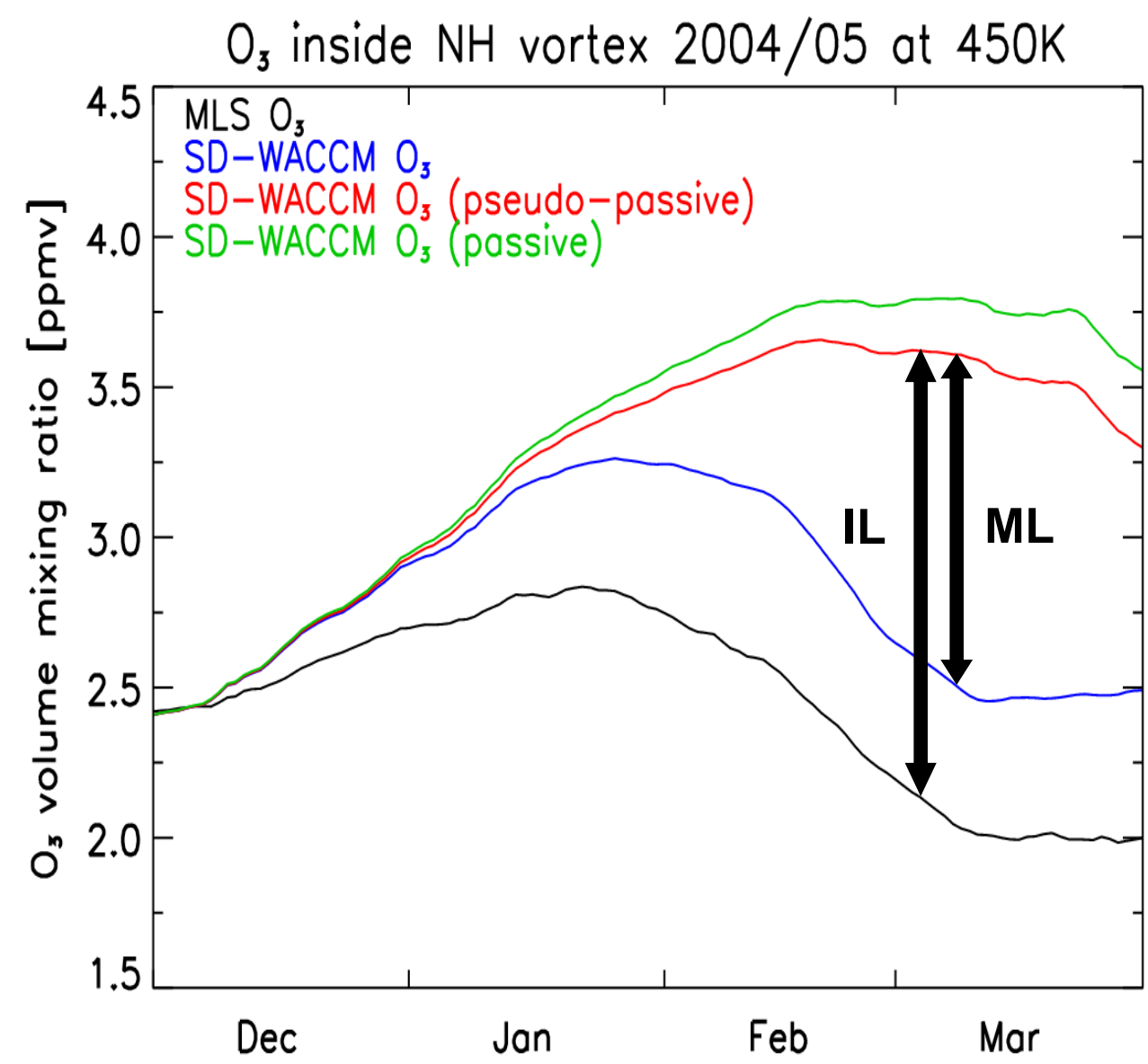


Figure 1: Evolution of observed ozone (black), modeled ozone (blue), modeled pseudo-passive ozone (red), and modeled passive ozone (green).

## DATA

- EOS MLS on Aura (since August 2004), version 2.2
- SD-WACCM (nudged daily with GEOS\* U, V, T), version 3548
- \*Goddard Earth Observing System, reanalysis, version 5

## INITIALIZATION

Global  $O_3$ , nitrous oxide ( $N_2O$ ), nitric acid ( $HNO_3$ ), hydrogen chloride (HCl), and water vapor ( $H_2O$ ) initialized with MLS data

- On 1 Dec: before first  $O_3$  loss occurs
- MLS data interpolated to SD-WACCM grid
  - Interpolation done on SD-WACCM pressure levels
  - Delaunay-Triangulation
  - Equal-area smoothing
- Cannot treat diurnal variations (e.g. chlorine monoxide (ClO))

## REFERENCES

- Jin, J. J., et al. (2006), *Geophys. Res. Lett.*, 33, L15801, doi:10.1029/2006GL026752.
- Manney, G. L., et al. (2006), *Geophys. Res. Lett.*, 33, L04802, doi:10.1029/2005GL024494.
- Rex, M., et al. (2006), *Geophys. Res. Lett.*, 33, L23808, doi:10.1029/2006GL026731.
- Rösevall, J. D., et al. (2008), *J. Geophys. Res.*, 113, D13301, doi:10.1029/2007JD009560.
- Santee, M. L., et al. (2008), *J. Geophys. Res.*, 113, D12307, doi:10.1029/2007JD009057.
- Singleton, C. S., et al. (2007), *J. Geophys. Res.*, 112, D07304, doi:10.1029/2006JD007463.

**Acknowledgments:** Work at University of Colorado was funded by NASA subcontract JPL 1350080. Work at the Jet Propulsion Laboratory, California Institute of Technology, was done under contract with the National Aeronautics and Space Administration.

**Contact:** brakebusch@lasp.colorado.edu

## COMPARISON OF MEASURED AND MODELED $O_3$ & $O_3$ LOSS

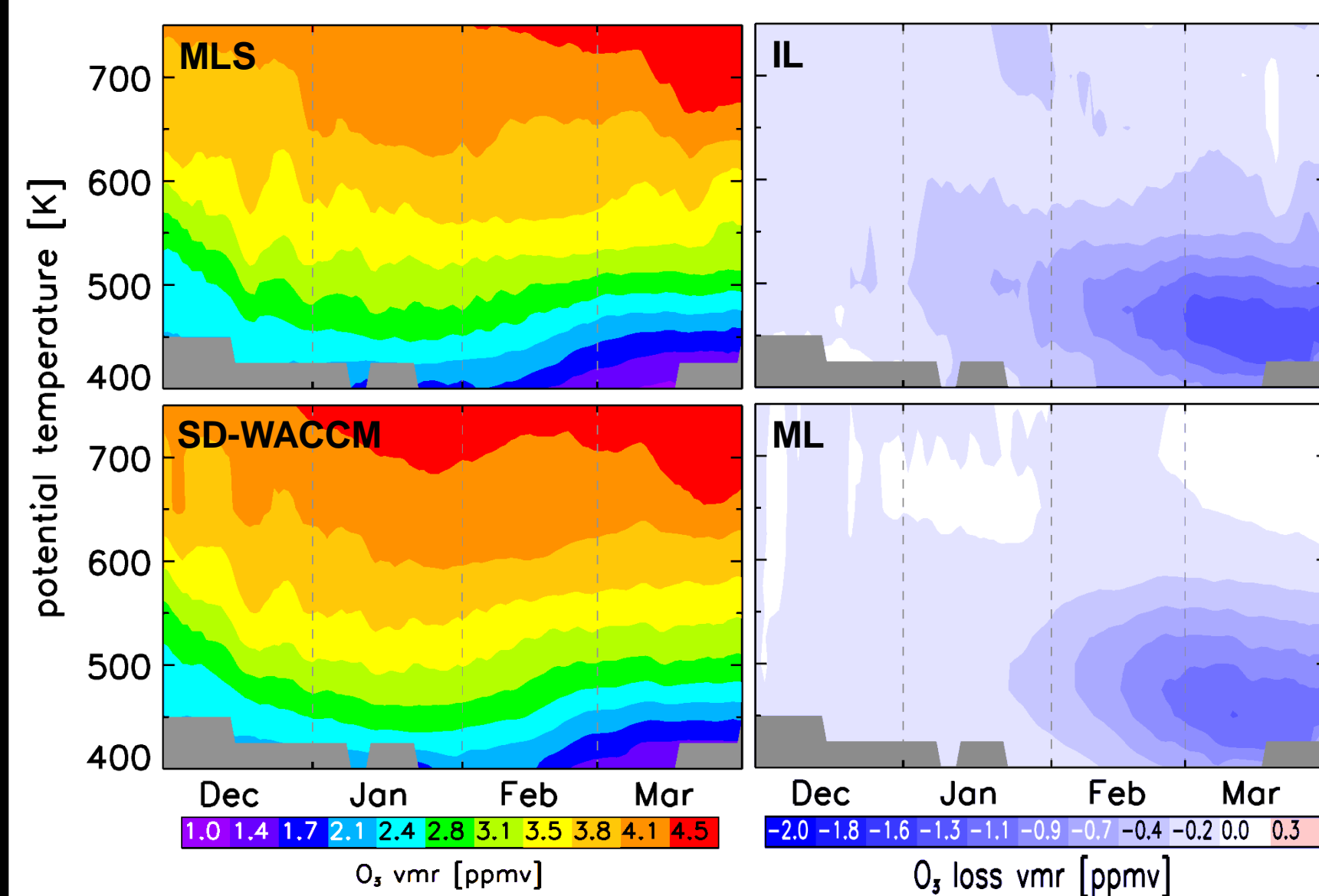


Figure 2: Evolution of vortex averaged ( $sPV > 1.6 \cdot 10^{-4} s^{-1}$ )  $O_3$  (left) from MLS (top) and SD-WACCM (bottom) and  $O_3$  loss (right) for IL (top) and ML (bottom). Compensation of errors in descent and/or mixing by errors in  $O_3$  loss (see below) leads to excellent agreement of  $O_3$  from MLS and SD-WACCM.

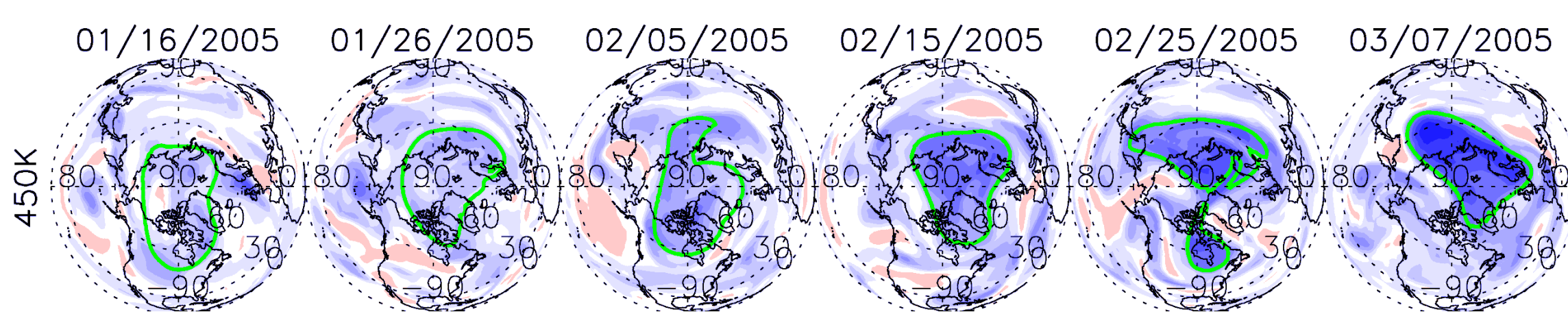


Figure 3: Spatial distribution of inferred  $O_3$  loss at 450K in 10day intervals throughout the season (same color bar as Fig. 2) with a green  $1.6 \cdot 10^{-4} s^{-1}$  sPV contour. Largest  $O_3$  loss of 2ppmv occurs at the end of the season.

Table 1: Comparison of shown  $O_3$  loss results (last column) with previous research.

Potential Temperature	Manney et al. [2006]	Jin et al. [2006]	Rex et al. [2006]	Rösevall et al. [2008]	Singleton et al. [2007]	MLS/WACCM
400K		0.8 ppmv	$1.6 \pm 0.3$ ppmv	0.7 ppmv	1.4 ppmv	0.6 ppmv
450K	1.2 - 1.5 ppmv	2.0 ppmv	$1.7 \pm 0.4$ ppmv	1.3 ppmv	2.2 ppmv	1.3 ppmv
500K	1.2 - 1.5 ppmv	2.1 ppmv	$1.1 \pm 0.4$ ppmv	0.8 ppmv	1.8 ppmv	1.0 ppmv
550K		1.2 ppmv	$0.6 \pm 0.3$ ppmv	0.5 ppmv	1.3 ppmv	0.5 ppmv
600K		0.6 ppmv		0.4 ppmv	0.6 ppmv	0.3 ppmv

## COMPARISON OF MEASURED AND MODELED $N_2O$

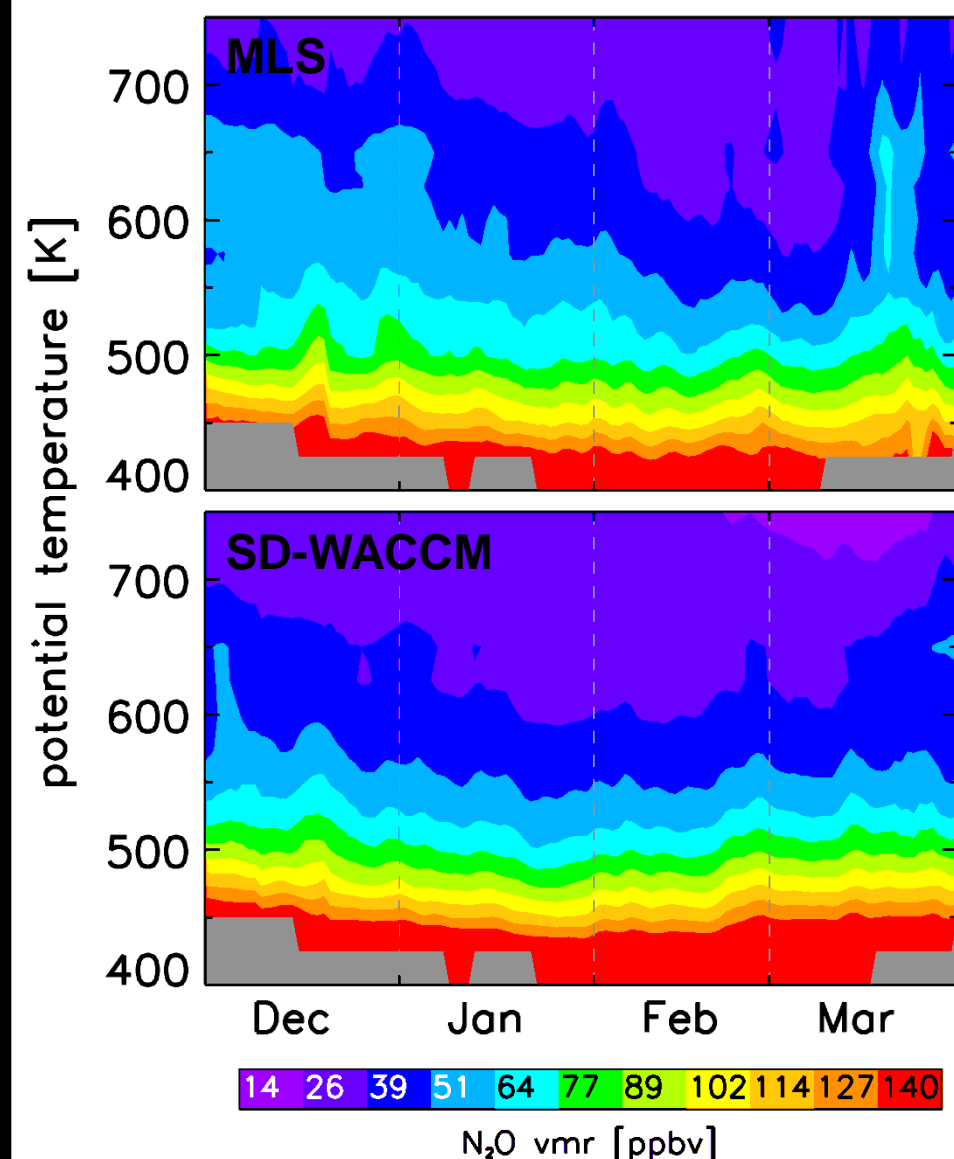


Figure 4 (left): Evolution of MLS (top) and SD-WACCM (bottom) vortex averaged  $N_2O$  ( $sPV > 1.6 \cdot 10^{-4} s^{-1}$ ). Differences indicate errors in SD-WACCM simulation of descent and/or mixing. However, no clear distinction between differences in descent and mixing across the vortex edge can be made.

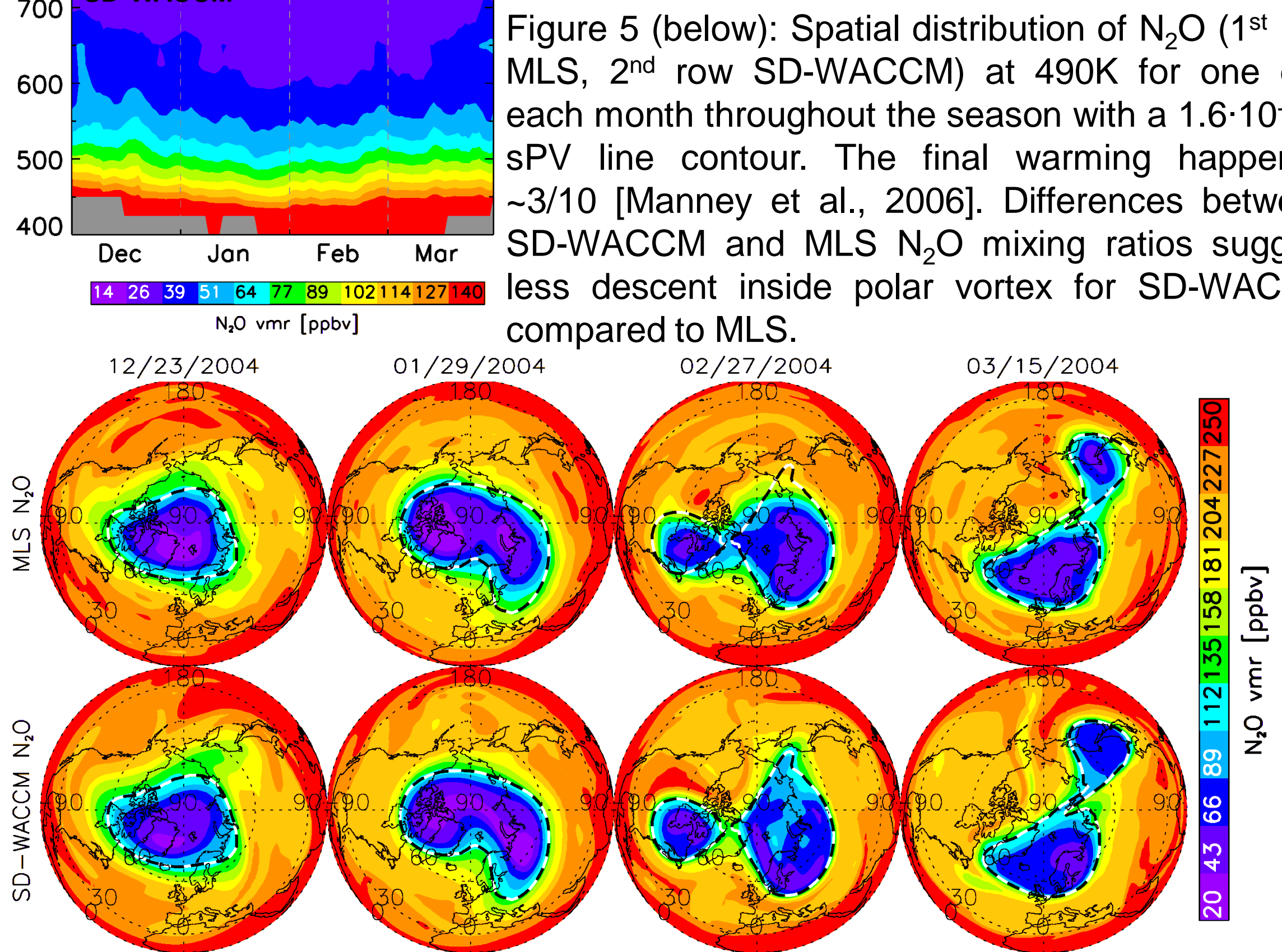


Figure 5 (below): Spatial distribution of  $N_2O$  (1st row MLS, 2nd row SD-WACCM) at 490K for one day each month throughout the season with a  $1.6 \cdot 10^{-4} s^{-1}$  sPV line contour. The final warming happened ~3/10 [Manney et al., 2006]. Differences between SD-WACCM and MLS  $N_2O$  mixing ratios suggest less descent inside polar vortex for SD-WACCM compared to MLS.

## RELATED CHEMICAL DIAGNOSTICS

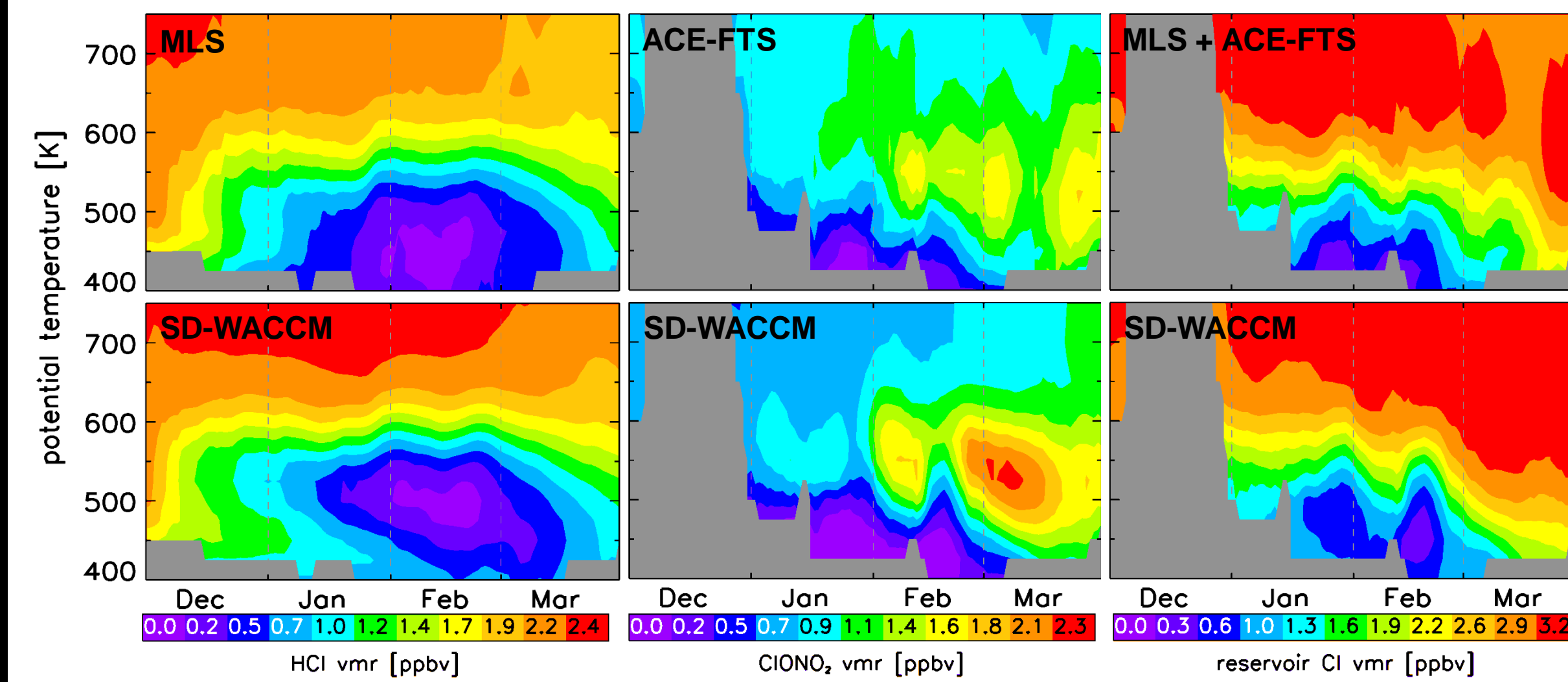


Figure 6: Evolution of observed (top row) HCl (left),  $ClONO_2$  (middle), their sum (right) and SD-WACCM respectively (bottom row) inside the polar vortex ( $sPV > 1.6 \cdot 10^{-4} s^{-1}$ ). Cl in reservoir species from SD-WACCM compares well with observations, suggesting the correct partitioning of chlorine between reactive forms and reservoirs.

## RELATED MICROPHYSICAL DIAGNOSTICS

Figure 7 (left): Evolution of polar vortex averaged ( $sPV > 1.6 \cdot 10^{-4} s^{-1}$ ) gas-phase  $HNO_3$  from SD-WACCM (bottom) compares well with MLS (top). Slight underestimates in the model are found later in the season below ~550K.

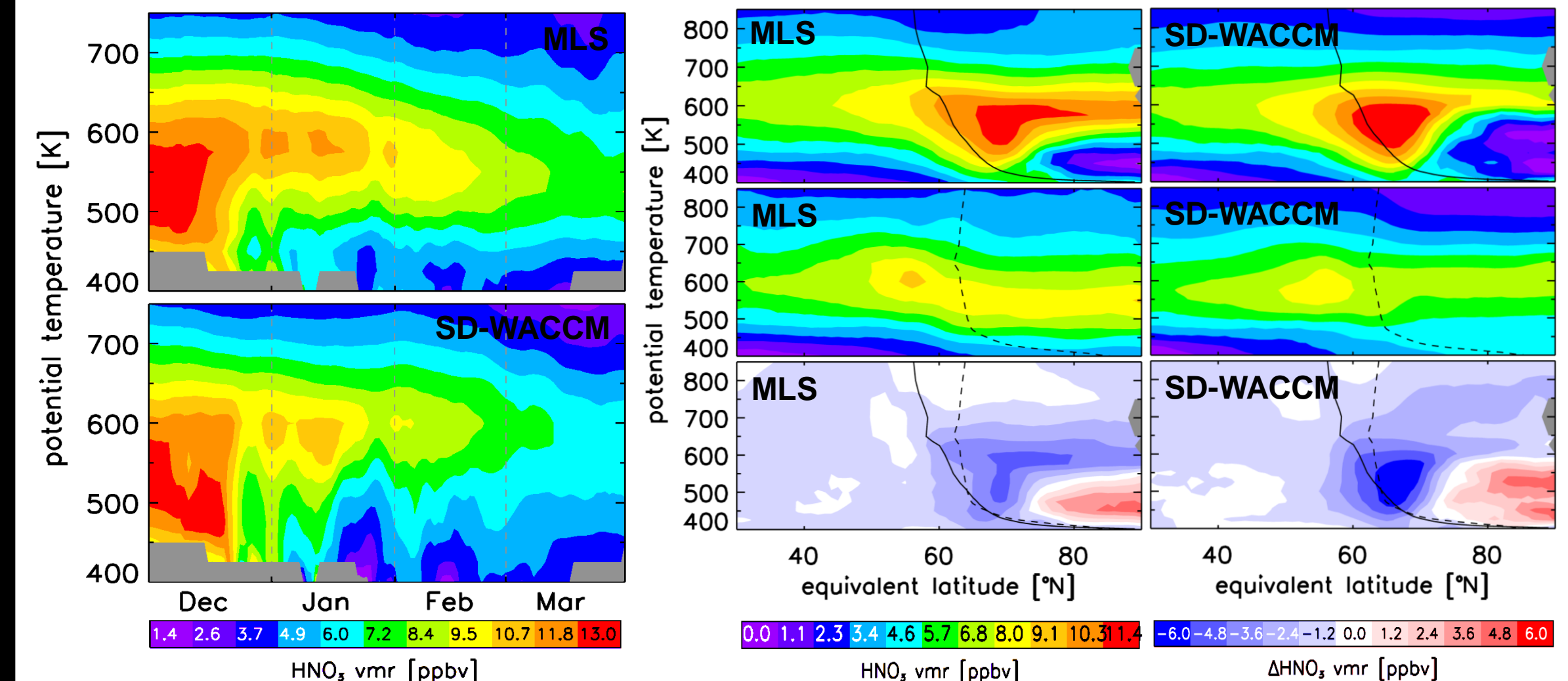


Figure 8 (right): Gas-phase  $HNO_3$  profiles from MLS (left) and SD-WACCM (right) on 1/23 (top) and 3/10 (middle), and 3/10 minus 1/23 (bottom).

Too much uptake of gas-phase  $HNO_3$  in SD-WACCM is consistent with too little  $ClONO_2$  (see Fig. 6). Reasonable  $O_3$  loss then suggests that PSC particle size distribution is shifted towards bigger radii (more uptake, same surface area).

## POLAR VORTEX EDGE

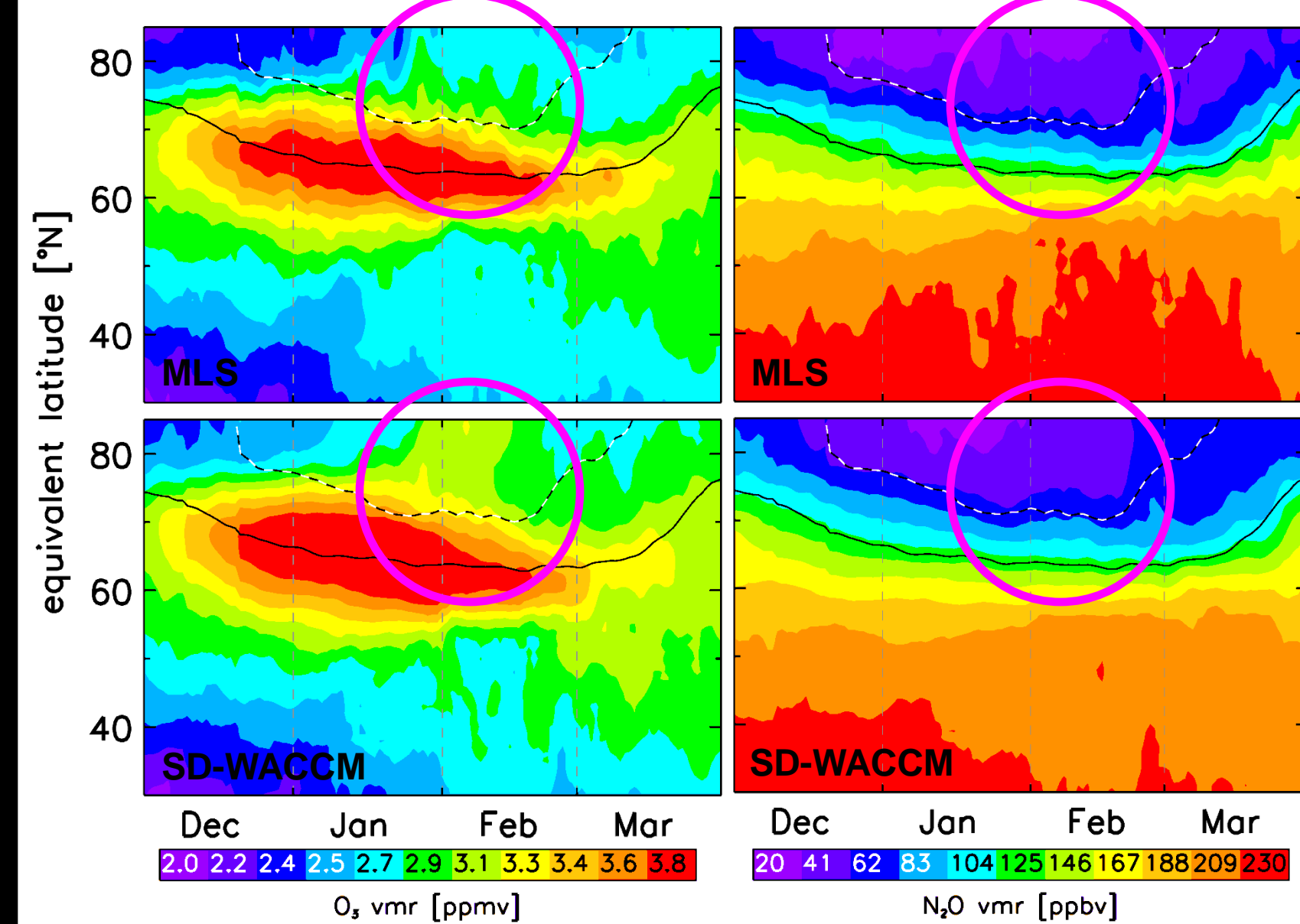


Figure 9: Evolution of MLS (top row)  $O_3$  (left) and  $N_2O$  (right) compared to SD-WACCM (bottom row) at 490K. SD-WACCM shows stronger mixing than MLS across polar vortex edge (solid  $1.6 \cdot 10^{-4} s^{-1}$  and dashed  $2.2 \cdot 10^{-4} s^{-1}$  sPV contours) in late Jan and Feb (circled). This enhances apparent inferred  $O_3$  loss at this time.

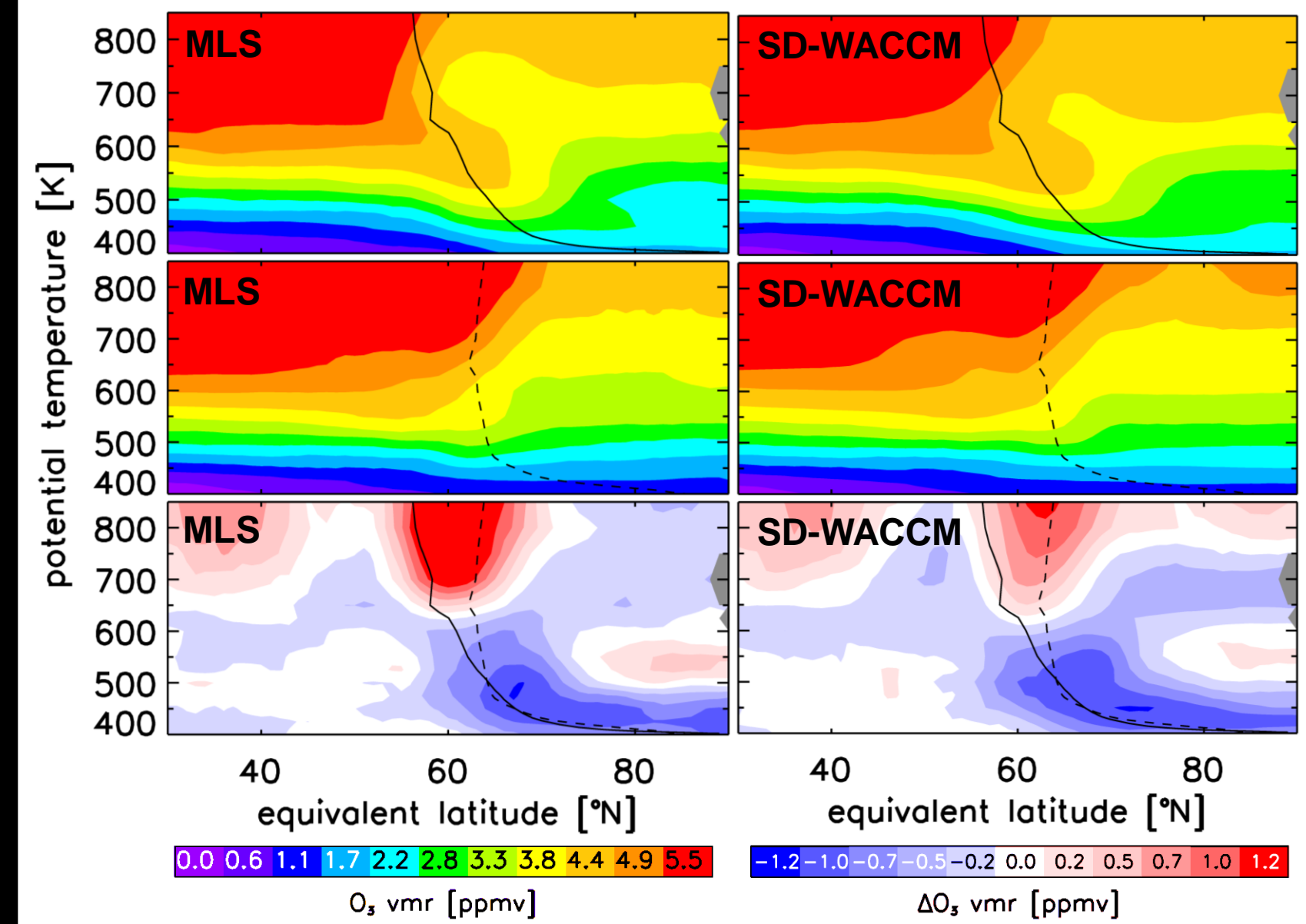


Figure 10:  $O_3$  profiles from MLS (left) and SD-WACCM (right) on 1/23 (top) and 3/10 (middle), and 3/10 minus 1/23 (bottom). Polar vortex edge as  $1.6 \cdot 10^{-4} s^{-1}$  sPV line contours. Biggest changes at polar vortex edge; changes are weaker in SD-WACCM than MLS.

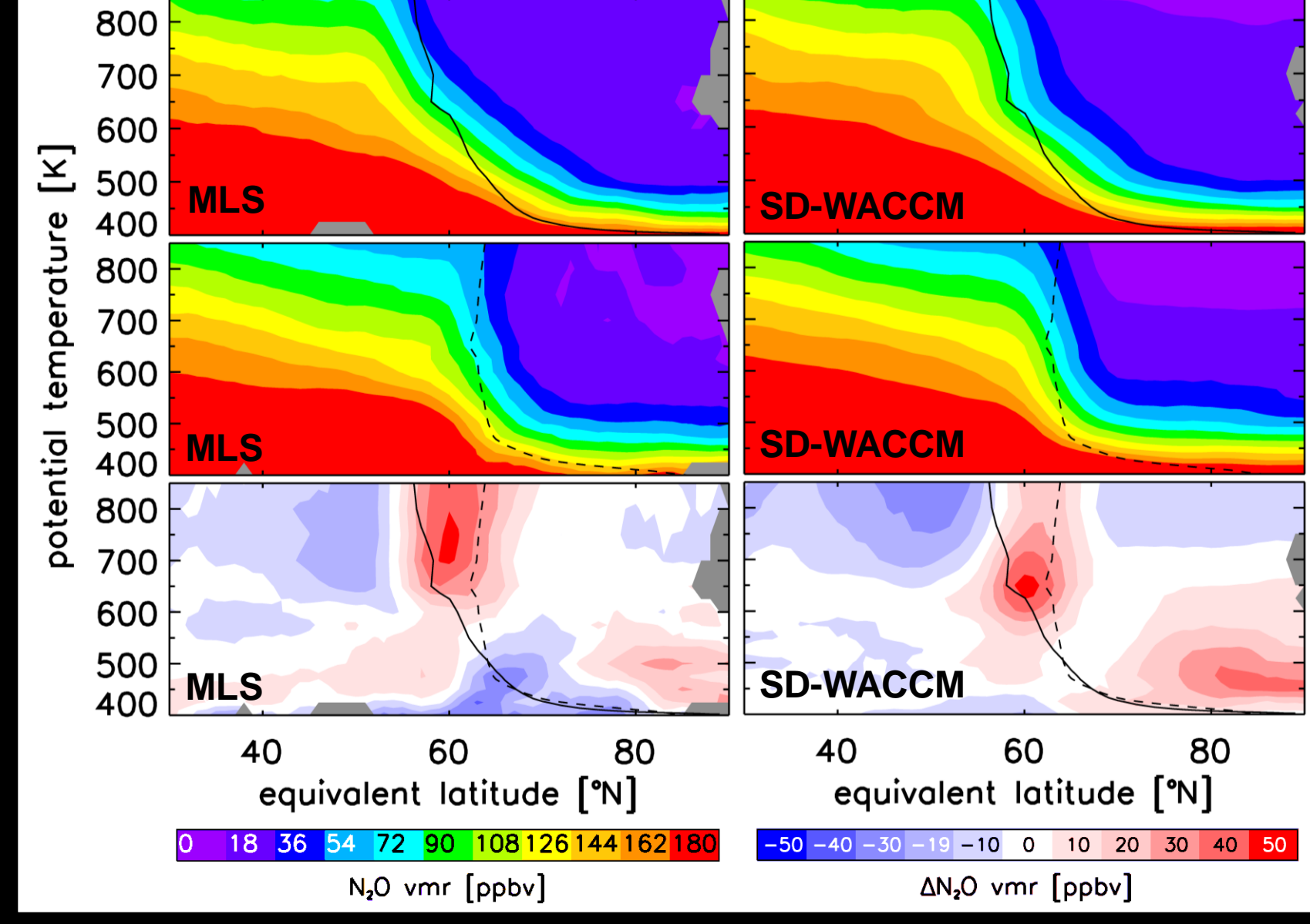


Figure 11: Same as in Fig. 10, but for  $N_2O$ . SD-WACCM and MLS compare well, but SD-WACCM shows larger increase near and inside the vortex edge below 700K. This could indicate too little descent and/or too much mixing.

## CONCLUSIONS

- SD-WACCM is valid for inferring  $O_3$  loss from observations
- More accurate simulation of  $O_3$  loss in WACCM requires further investigation of chlorine partitioning and PSC particle sizes
- Equivalent analysis for Antarctic winter needed to better investigate mixing and descent
- Future plans include  $O_3$  loss calculations for all Arctic and Antarctic winters since 2004